



Title	Microstructure and Mechanical Properties of Friction Stir Welded Pure Cu Plates
Author(s)	Sun, Yufeng; Xu, Nan; Morisada, Yoshiaki et al.
Citation	Transactions of JWRI. 2012, 41(1), p. 53-58
Version Type	VoR
URL	https://doi.org/10.18910/23160
rights	
Note	

The University of Osaka Institutional Knowledge Archive : OUKA

<https://ir.library.osaka-u.ac.jp/>

The University of Osaka

Microstructure and Mechanical Properties of Friction Stir Welded Pure Cu Plates[†]

SUN Yufeng*, XU Nan**, MORISADA Yoshiaki***, FUJII Hidetoshi***

Abstract

The process window for the friction stir welding of fully annealed commercial pure Cu was determined at an applied load of 1000kg, which includes a welding speed that ranged from 200 to 800 mm/min, and a rotation speed that ranged from 500 to 1300 rpm. In the stir zone of sound welds, a remarkably refined microstructure with the average grain size of 6.9 μm can be obtained by decreasing the rotation speed to 1000 rpm. However, the grain size becomes larger than the base metal when the rotation speed is higher than 1300 rpm. The stir zone may contain a structure composed of a high density dislocation cell or large developed annealing twin. The joints welded at a rotation speed less than 1300 rpm fractured in the base metal. However, the joints welded at a rotation speed higher than 1300 rpm fractured in the stir zone. The mechanism of the mechanical property changes in the Cu welds was proposed and clarified from the viewpoint of microstructural evolution.

KEY WORDS: (Friction stir welding) (Microstructure) (Mechanical property) (pure Cu)

1. Introduction

Friction Stir Welding (FSW) was invented by the Welding Institute of the UK in 1991 with the original purpose of the joining of Al and Al alloys, since the Al alloys are very difficult to weld by conventional fusion welding methods [1]. FSW is a solid state joining technique, in which a rotating tool is plunged into the work-pieces and traverse along the weld path. In this way, the rotating tools can plastically deform (stir) and transport the surrounding material from the front to the back of the tools. As a result, the work-pieces can be stirred together to form a joint [2, 3].

The welding of Cu has been a long-term project. Although Cu and Cu alloys can be joined by most of the commonly used methods such as gas welding, arc welding, resistance welding, brazing and soldering, the joining of Cu is usually difficult by conventional fusion welding methods because Cu has a thermal diffusivity of about 401 W/mK, which is almost the highest among all the metallic materials. For conventional fusion welding, higher heat input is required due to the high thermal conductivity of Cu. Oxidation and distortion of the Cu plates easily take place. In addition, after welding, very coarse grains are formed in the fusion zone, which results in a very low strength of the welds. With the development of the FSW technique and the very successful application of FSW to Al, the FSW technique has been developed further and extended for many other metallic materials, like Mg alloys, steel, Ti alloys, etc [4-9]. FSW of Cu has also been studied and reveals that the FSW technique is a very promising

method for the joining of Cu.

However, the FSW of Cu has not been well developed. Because the melting point of Cu is much higher than that of Al, much friction heat is generated during welding and the use of high temperature durable rotating tools is necessary. Up to now, there are only a few publications about the FSW of Cu and the mechanical properties of the joint cannot be comparable with that of the base metals [10-13]. Usually, the welded sample fractured in the stir zone during the tensile tests. In addition, the welding parameters and mechanical properties of the welds are greatly dependent on the heat treatment status of the Cu base metal. For example, when half work-hardened pure Cu (1/2H condition) was friction stir welded, a high applied load was necessary to obtain sound welds with a strength higher than that of the base metal [14]. As for work-hardened pure Cu (H condition), which was mainly strengthened by a high density of dislocations, additional rapid cooling, using cooling water, must be explored during the FSW process [15].

In this study, the FSW was applied to the welding of 2 mm thick pure Cu plates under a fully annealed condition (O condition). Various welding conditions over a wide range were tried in order to obtain the process window for the FSW of pure Cu. After welding, the relationship between the microstructure evolution and mechanical properties of the FSW processed specimen were investigated and discussed.

2. Experimental

[†] Received on June 18, 2012
^{*} Specially Appointed Associate Professor
^{**} Graduate Student
^{***} Professor

Transactions of JWRI is published by Joining and Welding Research Institute, Osaka University, Ibaraki, Osaka 567-0047, Japan

The Cu plates used in this study were as-received commercial pure Cu under a fully annealed state and had dimensions of 200 mm long, 50 mm wide and 2 mm thick. During the FSW process, two Cu plates were put together and clamped tightly. The rotating tools made of SKD61 were used and were inclined 3° during the welding process. The welding speed was varied between 200-800 mm/min, the rotation speed ranged from 600 to 1350 rpm and the applied load was fixed at 1000 kg. To prevent the oxidation of the Cu, the FSW processes were carried out with argon gas flowing around the rotating tools.

After welding, optical microscopy (OM) was used to characterize the macrostructure of the joints. The samples for the OM observation were cross-sectioned perpendicular to the welding direction, polished and then etched with a solution of iron chloride. The electron backscattered diffraction (EBSD) measurements were carried out using a JEM 5200 scanning electron microscope (SEM) with a TSL orientation imaging system. The microstructures in the stir zone as well as the base metal were characterized by transmission electronic microscopy (TEM). For the TEM sample preparation, thin plates were twin-jet electro-polished to make electron beam transparent thin films using a solution of $\text{HPO}_4:\text{CH}_3\text{OH}:\text{H}_2\text{O}=1:1:2$ at 5 V and 0°C . The thin films were observed using a Hitachi 800 TEM at 200 kV. The Vickers hardness profiles of the joints were measured along the center line of the cross-section and perpendicular to the welding direction using a Vickers indenter with a load of 980 mN and dwell time of 15 s. The tensile tests were carried out using an Instron-type testing machine with a crosshead speed of 1 mm/min. The tensile direction was perpendicular to the welding direction.

3. Results and Discussion

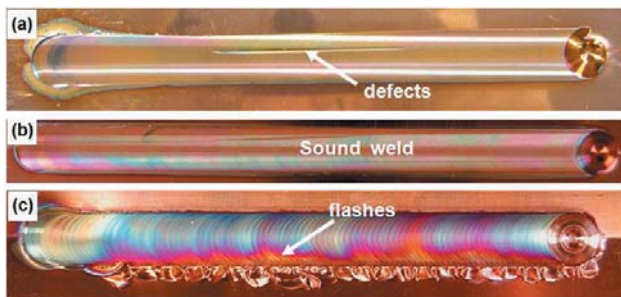


Fig. 1 Three kinds of appearance of the FSW processed Cu welds. (a) defects; (b) sound weld; and (c) superfluous flash

For all the Cu plates welded at the different welding conditions, three kinds of phenomena might generally appear according to the appearance of the welded samples. **Figure 1** shows the typical three kinds of weld appearances. **Figure 1(a)** shows the sample with defect formation due to an insufficient heat input. **Figure 1(b)** shows the sound sample with a clean surface and without any defects. **Figure 1(c)** shows the sample with superfluous flash due to too high heat input.

According to the weld appearance of the Cu obtained at the different welding parameters, the process window for the welding of Cu can be drawn as shown in **Figure 2**. This shadow area indicates the possible welding conditions for the FSW of Cu. For the place below this shadow area, it means that the heat input is not high enough for sound welds and usually defects will form in the joint. However, for the area above this shadow area, the heat input is too high and therefore the temperature rise is high. As a result, too much flash will form and a coarse microstructure will form in the joints. Compared with the process window for the FSW of pure Al, the process window of Cu is narrower because Cu has a much higher melting point than that of Al. However, the process window of annealed Cu is much larger than that of the work-hardened Cu, in which annealing softening easily occurs and makes it difficult to obtain sound welds.

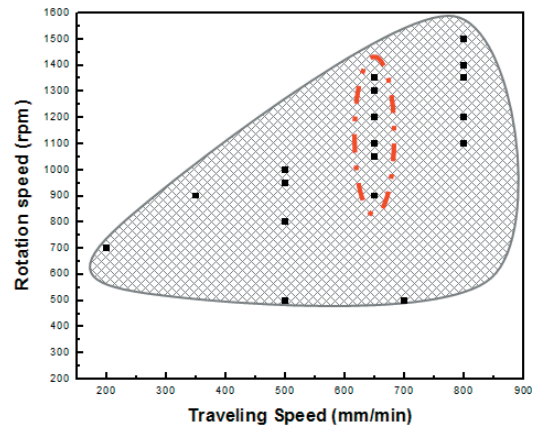


Fig. 2 Process window for the FSW of pure Cu

To reveal the effects of the heat input on the microstructure and mechanical properties of the Cu welds, the microstructural evolution and mechanical properties of the selected samples welded at various rotation speeds were investigated. However, the welding speed and applied load were constant at 650 mm/min and 1000 kg, respectively.

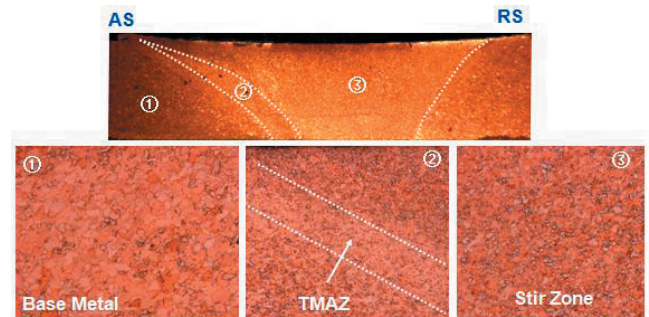


Fig. 3 The typical cross-sectional microstructure of the FSW processed pure Cu

For all the samples welded at the different rotating speeds, three kinds of specific zones in the joints can

generally be observed, namely, the stir zone, the thermo-mechanically affected zone (TMAZ), and the base metal. However, the heat affected zone (HAZ) is not obvious. As a typical example, **Figure 3** shows the macrostructure of the joint after the FSW process and the specific zones are separated by the white dotted line. Both the base metal and the stir zone have an equiaxial grain structure. Between the base metals and the stir zone, the TMAZ characterized by an elongated grain structure can be observed.

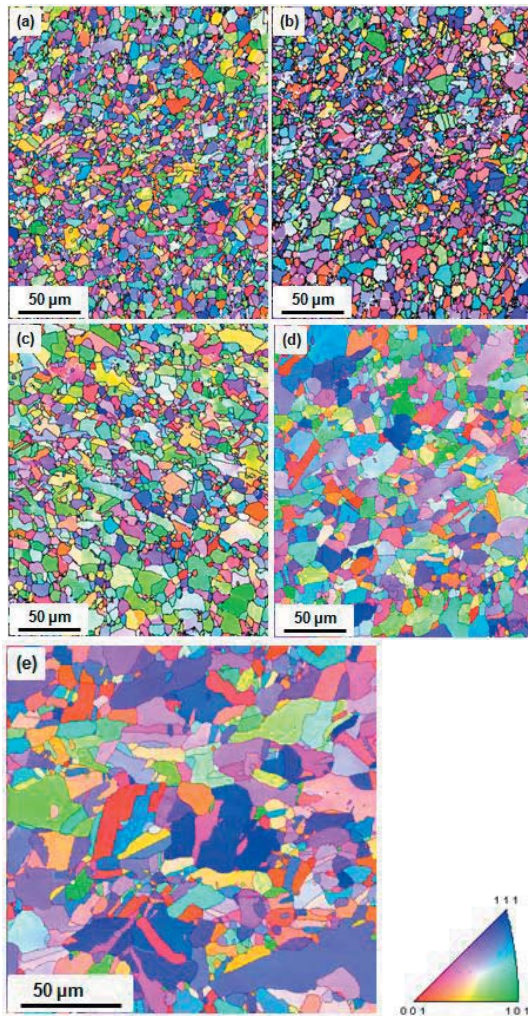


Fig. 4 EBSD map showing the microstructure of the stir zone of the welds obtained under different welding conditions. (a) 1000 rpm; (b) 1100 rpm; (c) 1200 rpm; (d) 1350 rpm and (e) base metal.

Figure 4 shows the EBSD maps revealing the microstructure in the center of the stir zone welded at different rotation speeds, together with the EBSD map of the base metal. In the maps, only the high angle boundary is indicated by the black lines. The stir zones of all the welds show an equiaxial grain structure, which implies that dynamic crystallization occurred during the FSW process. It is also observed that the average grain size increases with the increasing rotation speed. When the

rotation speed increased to 1350 rpm, the average grain size increased to about 16.9 μm , which is larger than 14.9 μm of base metal. After the nucleation of the dynamic recrystallization, the newly formed grains experienced a period of grain growth. The higher heat input caused by the high rotation speed might accelerate the growth rate to form the coarse grain structure. The average grain size of the welds and the base metal are summarized in **Table 1**.

Table 1. The average grain size obtained under different welding conditions

Rotation Speed	1000 rpm	1100 rpm	1200 rpm	1350 rpm	BM
Av.GS (μm)	6.9	7.0	9.9	16.9	14.9

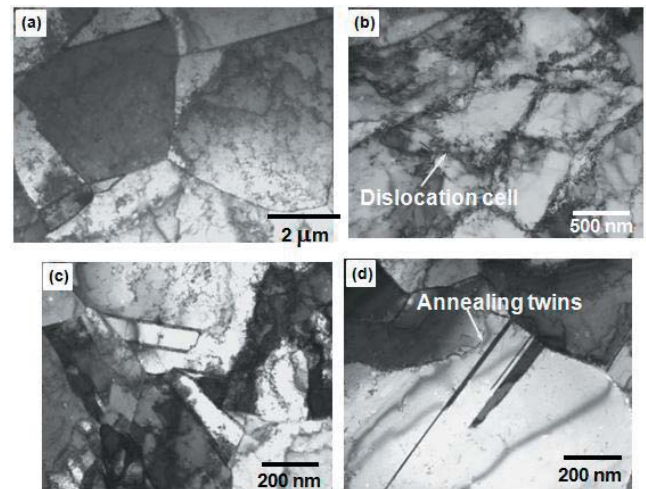


Fig. 5 TEM images showing the microstructure of the (a) base metal; and (b-d) the stir zone

Figure 5 shows the TEM images taken in the stir zone of the sample welded at 1000 rpm. For comparison, the TEM image of the base metal was also included. The TEM image of the base metal shows that the microstructure is dominated by equiaxial grains. Although the base metal was received in the annealed state, more or less dislocation can still be found, however, with a very low density as shown in **Figure 5(a)**. The microstructure in the stir zone shows obvious different features. One is the high density of the dislocation cells as shown in **Figure 5(b)**. This figure shows the formation of dislocation cells within the Cu grains. This indicates that the slip deformation mode and the dislocation cells will probably transform into subgrains if more deformation is introduced. Another feature is the formation of annealing twins. The annealing twins were generated at the grain boundary and developed into the grains. The annealing twins can also accommodate a part of the deformations. **Figure 5(c)** shows the formation of the annealing twins, together with dislocations with a relatively low density. **Figure 5(d)** shows another kind of grains with formation of annealing twins. In addition, the dislocations can hardly be found.

After welding, the Vickers hardness was used to evaluate the mechanical properties of the joints. The

Vickers hardness was tested along the center line of the cross-section of the sample across the joints. **Figure 6** shows the hardness profile of the joints welded under different welding conditions. Generally, the hardness increased with the decreasing tool rotation speed, or refinement of the grain size. When the rotation speed is less than 1200 rpm, the hardness in the stir zone is higher than that of the base metal. When the rotation speed is higher than 1200 rpm, the stir zone hardness is lower than that of the base metal. It is worthy to note that, the hardness distribution along the weld centerline is not symmetric and the lowest hardness in the stir zone for all the samples is located in an area inclined to the advancing side, which is indicated in the shadow rectangle area shown in **Figure 6**. Although according to some publications, the temperature distribution about the weld centerline is symmetric and therefore the hardness distribution should be symmetric [16], Maeda et al. and Liu et al. found that the temperature distribution around the rotating tool was not symmetric [17,18]. Compared with the position on the retreating side, the position having the same distance from the centerline on the advancing side shows a higher temperature rise during the welding process. As a result, the lowest hardness in the stir zone is generally located in an area inclined to the advancing side due to the relatively higher heat input.

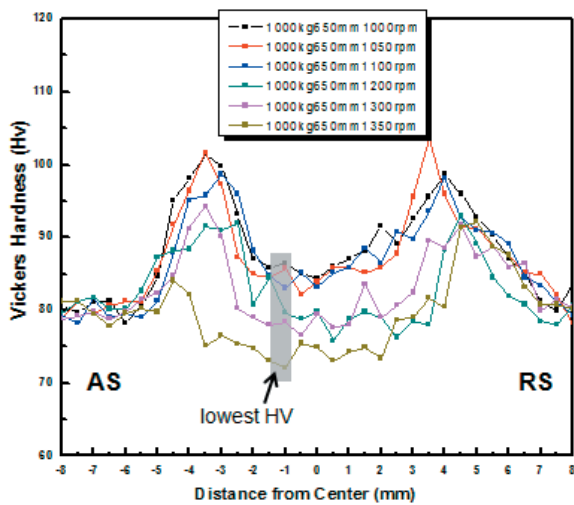


Fig. 6 The hardness profile of the FSW processed welds obtained under different welding conditions (AS: advancing side; RS: retreating side)

In the present study, the hardness distribution of the fully annealed Cu joints is quite different from that of the work-hardened Cu joints. In the work-hardened Cu joints, the hardness reduction usually occurs in the stir zone, even though the grain size in the stir zone is remarkably smaller than that of the base metal. This phenomenon has been reported previously and it was believed that the annealing exerted a larger effect than the grain refinements on the mechanical properties of the Cu joints [14, 15]. As for the fully annealed Cu joints, the hardness

is mainly dominated by the grain size. It is interesting to note that the hardness in the TMAZ is remarkably larger than that in the stir zone. That is because the temperature rise in the stir zone is higher than that in the TMAZ, and the deformed grains experienced a serious recovery and dynamic recrystallization process. However, in the TMAZ, the grains were deformed, elongated, but still with a high density of dislocations.

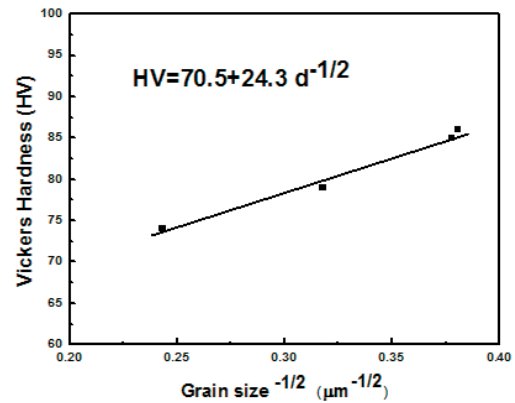


Fig. 7 The Hall-Petch relationship obtained for the stir zone of the FSW processed Cu obtained at different rotation speeds

For conventional polycrystals with grain sizes ranging from several to hundreds of micrometers, the hardness and the strength dependences on the mean grain size can be described by the Hall-Petch relations:

$$\sigma_y = \sigma_0 + k \cdot d^{-1/2} \quad \text{or} \quad HV = HV_0 + k \cdot d^{-1/2}$$

where σ_y and HV are the yield stress and hardness, respectively; d is the average grain size, and σ_0 , HV_0 and k are material constants. The Hall-Petch relations reveal that decreasing the grain size can increase the tensile strength of the materials. In the present study, the relationship between hardness and the average grain size was used to verify the Hall-Petch relations for the FSW of Cu. In the tensile tests, the welded sample fractured at different locations including the stir zone, HAZ and base metal, where the average grain size can not be precisely measured. Therefore, the measurement of hardness was used to investigate the feasibility of the Hall-Petch relations for the FSW of Cu. The relationship of the Vickers hardness and the average grain size measured at the geometric center of the stir zone was plotted in **Figure 7**. The Hall-Petch equation can therefore be extrapolated as

$$HV = 70.5 + 24.3 \cdot d^{-1/2}$$

It was found that the hardness and average grain size for all the welded joints follow the Hall-Petch relation.

Figure 8 shows the tensile stress-strain curves for the specimens obtained under different welding conditions, together with that of the as-received pure Cu. For all the specimens obtained under the different welding conditions, the yielding points and fracture strength during the tensile tests are similar to each other and similar to that of the

base metal, which is about 160 MPa and 245 MPa, respectively. In addition, the specimens welded at a rotation speed of less than 1300 rpm show an engineering strain of about 45%, equivalent to that of the base metal. However, the specimens welded at a rotation speed of 1300 rpm or higher show a lower plastic strain. The plastic strain decreased with the increasing rotation speed, or the increase of the average grain size in the stir zone.

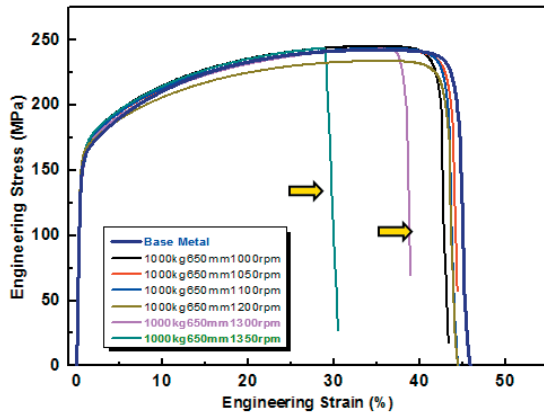


Fig. 8 The tensile tests curves for the FSW processed Cu obtained at different rotation speeds

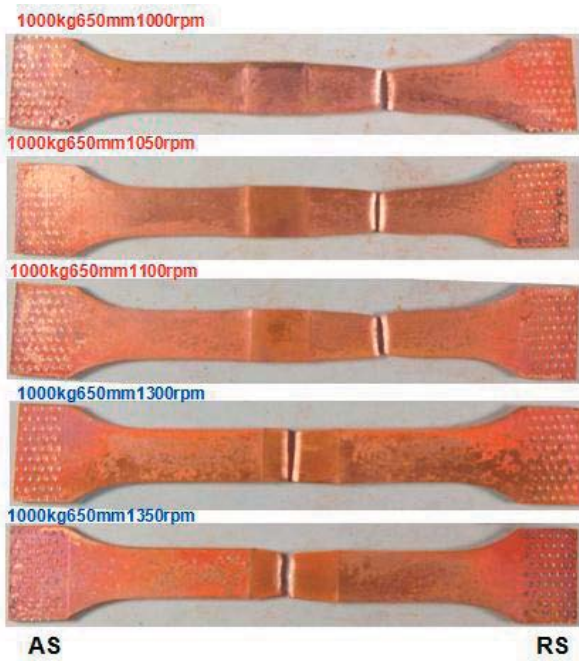


Fig. 9 The appearance of the fractured tensile specimen welded at different rotation speeds (AS: advancing side; RS: retreating side)

Figure 9 shows the typical appearance of the fractured specimens, which are welded at different rotation speeds from 1000 to 1350 rpm. For all the specimens welded at a rotation speed of 1100 rpm or less, the fracture occurred in the base metal far from the stir

zone. This is because the average grain size in the stir zone is smaller than that of the base metal due to the lower heat input. The strength in the stir zone is assumed to be higher than that of the base metal, although tensile tests of miniature specimens for the stir zone were not carried out [19]. However, for the specimens welded at a rotation speed of 1300 rpm or higher, the fracture is located in the stir zone but slightly inclined to the advancing side. The higher rotation speed resulted in higher heat input and therefore the rapid grain growth in the stir zone. The average grain size is larger than that of the base metal, but has a lower strength than that of the base metal. From the hardness profile shown in Figure 6, it was found that all the specimens fractured at the locations with the lowest hardness value in the samples, which matches well with the hardness measurement.

4. Conclusions

In this study, the fully annealed commercial purity Cu plates with thickness of 2 mm were FSW processed with different welding parameters including the changes in the welding speed and rotation speed. The microstructure evolutions in the stir zone perpendicular to the welding direction were characterized and the mechanical properties of the welded joints were evaluated. Based on these descriptions, the following conclusions were obtained.

- (1) The optimum friction stir welding condition for cp-Cu was obtained.
- (2) The FSW process introduces a microstructure refinement in the stir zone at a rotation speed less than 1200 rpm, together with the formation of annealing twins and high density dislocations. However, a rotation speed of higher than 1200 rpm results in a coarser grain structure.
- (3) Most of the welded specimens fractured in the base metal. However, when the rotation speed was increased to 1300 rpm, the welded specimen fractured in the stir zone.

Acknowledgement

The authors wish to acknowledge the financial support of the Japan Science and Technology Agency (JST) under Collaborative Research Based on Industrial Demand “Heterogeneous Structure Control: Towards Innovative Development of Metallic Structural Materials”, a Grant-in-Aid for the Cooperative Research Project of National Wide Joint-Use Research Institute, the Global COE Programs from the Ministry of Education, Sports, Culture, Science, and a Grant-in-Aid for Science Research from the Japan Society for Promotion of Science and Technology of Japan, Toray Science Foundation, ISIJ Research Promotion Grant, and Iketani Foundation.

References

- [1] W. M. Thomas, E.D. Nicholas, J.C. Needham, International Patent Application No. PCT/GB92/02203 (1991).
- [2] R. S. Misha, Z. Y. Ma. Mater. Sci. Eng, R 50 (2005) 1-78.
- [3] R. Nandan, T. Debroy, H.K.D.H. Bhadeshia, Prog. Mater. Sci, 53 (2008) 980-1023.
- [4] Z. Y. Ma, Metall.Mater.Trans A, 39 (2008) 642-658.
- [5] Y. S. Sato, H. Kokawa, M. Enomoto, Metall.Mater.Trans. A, 30 (1999) 2429-2437.
- [6] L. Commin, M. Dumont, J. E. Masse, Acta Mater, 57 (2009) 326-334.
- [7] L. Cui, H. Fujii, N. Tsuji, K. Nogi, Scripta Mater, 56 (2007) 637-640.
- [8] H. Fujii, Y. F. Sun, H. Kato, K. Nakata. Mater. Sci. Eng. A, 527 (2010) 3386-3391.
- [9] Y. Miyano, H. Fujii, Y. F. Sun, Y. Katada, S. Kuroda, O. Kamiya. Mater. Sci. Eng A, 528 (2011) 2917-2921.
- [10] T. Sakthivel, J. Mukhopadhyay. J. Mater. Sci, 42 (2007) 8126-8129.
- [11] W. B. Lee, C.Y. Lee, W.S. Chang, Mater. Lett, 59 (2005) 3315-3318.
- [12] G. M. Xie, Z. Y. Ma, L. Geng. Scripta Mater, 57 (2007) 73-76.
- [13] H. J. Liu, J. J. Shen, Y. X. Huang, Sci. Technol, Weld. Join, 14 (2009) 577-583.
- [14] Y. F. Sun, H. Fujii. Mater. Sci. Eng. A, 527 (2010) 6879-6886.
- [15] P. Xue, B. L. Xiao, Q. Zhang and Z.Y. Ma. Scripta Mater, 64 (2011) 1051-1054.
- [16] W. Tang, X. Guo, J. C. McClure, L. E. Murr, A. Nunes. J. Mater. Process. Manuf. Sci., 7 (1998) 163-172.
- [17] M. Maeda, H. J. Liu, H. Fujii and T. Shibayanagi. Welding in the World, 49 (2005) 69-75.
- [18] H. Liu, H. Fujii, M. Maeda, K. Nogi. J. Mater. Sci. Lett., 22 (2003) 441-444.
- [19] W. T. Anthony, I. B. Michael. Philo. Mag., 28 (2010) 301-308.